

molybdenum bronze directly, whereas that of the electrolytic reduction is not. Experiments to elucidate the mechanism are now being done.

Figure 3 shows a scheme using a combination of the 'electrochemical mode' and the 'photon mode' in a MoO<sub>3</sub> thin film to achieve a display device, for example. Starting with a colourless MoO<sub>3</sub> film (stage A), it is slightly blued by cathodic polarization (electrochemical mode) to generate a visible-light-sensitive material (stage B). Then the desired pattern is written on it by visible light irradiation (photon mode, stage C). This pattern is easily erased at will either to the pretreated stage (stage B) or to the initial stage (stage A) by controlling the time for anodic polarization, and the film can be used repeatedly. □

Received 21 August; accepted 3 December 1991.

1. Deb, S. K. *Phil. Mag.* **27**, 801-822 (1973).
2. Deb, S. K. *J. appl. Phys.* **37**, 4818-4825 (1966).
3. Yao, J. N., Loo, B. H. & Fujishima, A. *Ber. Bunseng. Phys. Chem.* **94**, 13-17 (1990).
4. Colton, R. J., Guzman, A. M. & Rabalais, J. W. *Acct. Chem. Res.* **11**, 170-176 (1978).
5. Fleisch, T. H. & Mains, G. J. *J. chem. Phys.* **76**, 780-786 (1982).
6. Shigesato, Y. *Jap. J. appl. Phys.* **30**, 1457-1462 (1991).
7. Faughnan, B. & Crandall, R. S. *Appl. Phys. Lett.* **31**, 834-836 (1977).
8. Kitao, M., Yamada, S., Hiruta, Y., Suzuki, N. & Urade, K. *Appl. Surf. Sci.* **33/34**, 812-817 (1988).

## Tropical stratospheric circulation deduced from satellite aerosol data

Charles R. Trepte & Matthew H. Hitchman

Department of Meteorology, University of Wisconsin-Madison, 1225 West Dayton Street, Madison, Wisconsin 53706, USA

**THE dispersal of volcanic material from large tropical eruptions provides insight into the circulation of the lower stratosphere. Here we infer stratospheric motions from zonal mean cross-sections of satellite observations of the aerosol layer taken during 1979-81 and 1984-91. By examining the aerosol distribution following volcanic eruptions in the tropics, we find that poleward transport occurs readily at altitudes within a few kilometres above the tropopause, whereas in the altitude range of 21-28 km, aerosols tend to remain within 20° of the Equator. We further deduce that the aerosol distribution in this upper regime is controlled by the phase of the quasi-biennial oscillation. When the easterly shear is present, aerosols are lofted over the Equator, whereas when the westerly shear is present, descent relative to the mean stratospheric circulation occurs over the Equator. From the aerosol distributions, we suggest that the tropical stratosphere may be regarded as a temporary reservoir for trace constituents entering the stratosphere through the tropical tropopause.**

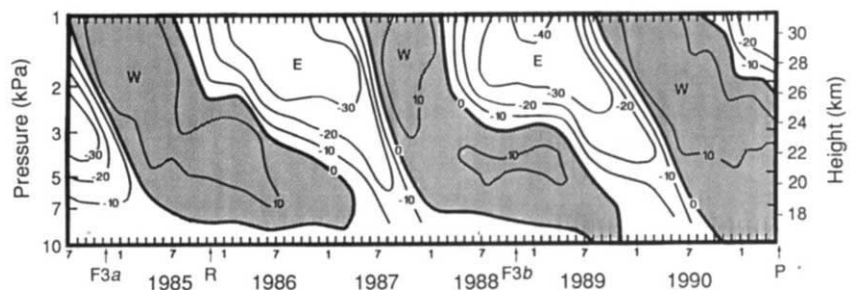
Stratospheric sulphate aerosols, primarily the byproduct of volcanic eruptions, have long been a focus of study<sup>1</sup>. They can influence the climate by altering the distribution of radiative heating and may affect the ozone layer by liberating active

chlorine and repartitioning odd-nitrogen species<sup>2</sup>. Here we use their distribution to deduce the circulation in the lower stratosphere. This circulation determines how air enters the stratosphere from the troposphere, and hence how trace constituents become distributed throughout the ozone layer.

From consideration of the water-vapour budget<sup>3</sup>, the column ozone distribution<sup>4</sup>, the radiative budget<sup>5</sup>, the dispersal of radioactive tracers<sup>6,7</sup> from bomb tests in the 1950s and 60s, and the pattern of diminution of solar radiation at the surface<sup>8</sup> after the eruption of Mount Agung in March 1963, the following pattern of mean stratospheric circulation has emerged and is now known as the Brewer-Dobson circulation. Air enters through the tropical tropopause. Some air travels poleward within a few kilometres of the tropopause and re-enters the troposphere in the extratropics, with the transport being stronger into the winter hemisphere. In the middle and upper stratosphere, air ascends further in the sunlit portion and descends over the winter pole. The circulation in the tropical lower stratosphere is dominated by a quasi-biennial oscillation (QBO) in zonal wind and temperature<sup>9</sup>. Figure 1 shows the variation of monthly mean zonal wind at Singapore for the period July 1984 to May 1991. The meridional circulation associated with the QBO, however, has only been estimated from theory and numerical models<sup>10-12</sup>. We have examined satellite estimates of the ratio of aerosol to Rayleigh extinction near 1 μm (refs 13, 14) from the stratospheric aerosol and gas experiments (SAGE I and II)<sup>13,15</sup> for the periods 1979-81 and 1984-91, respectively. Here we present sample distributions of sulphate aerosols and deduce the associated mean meridional circulation during two phases of the QBO (Fig. 3).

Detailed temperature measurements taken during November 1978 to May 1979 allow the QBO structure to be represented in terms of zonal mean potential vorticity (PV)<sup>16</sup>. PV can be regarded as a measure of the inertial and static stability of the air<sup>17</sup>. Where the gradient of PV is strong, the transport of constituents across that gradient will be inhibited<sup>18</sup>. The zonal mean distribution of PV is controlled by the absorption of gravity and planetary waves, the mean meridional circulation and radiative processes<sup>19</sup>. Figure 2 shows the distribution of normalized PV for early November 1978, defined as  $-(f/|f|)(1/r)\vec{v}M$ , where  $f$  is the Coriolis parameter,  $r$  is the distance to the Earth's rotation axis, and  $\vec{v}M$  is the zonal mean angular momentum gradient evaluated at constant potential temperature<sup>16</sup>. At this time, descending westerlies near 35 km associated with the equatorial semiannual oscillation<sup>16</sup> overlaid QBO easterlies in the layer 24-32 km, which in turn overlaid QBO westerlies below 24 km. Near 30 km, PV contours are spread out about the Equator and close together near 20° N and S. This pattern is compatible with easterly wave driving centred over the Equator with attendant divergent meridional flow into the subtropics. Near 22 km and 38 km, PV contours are pinched together over the Equator and the gradient is large near 10° N and S, a pattern which is compatible with westerly wave driving centred over the Equator and convergent meridional flow. In agreement with expectations from theory and models<sup>10-12</sup> this PV pattern is compatible with ascent over the Equator in easterly shear and descent relative to the mean stratospheric circulation over the

FIG. 1 Time-altitude section of monthly mean zonal wind component at Singapore (1°N, 104°E) for July 1984 to May 1991, adapted from ref. 24, showing the quasi-biennial oscillation in the equatorial lower stratosphere, contour interval 10 m s<sup>-1</sup>. Marked times R, P, F3a and F3b are the eruptions of Mounts Ruiz and Pinatubo and the aerosol cross-sections in Fig. 3a, b.



Equator in westerly shear. Near 20° N and S, vertical divergence occurs near the level of maximum equatorial easterlies. We use this model of the QBO meridional circulation together with the observed equatorial winds in Fig. 1 to interpret the aerosol distributions.

Two sections of aerosol extinction ratio during boreal autumn typify the descending westerly (Fig. 3a) and easterly (Fig. 3b) phases of the QBO. Values increase rapidly above the tropopause and peak over the Equator. Within a few kilometres above the tropopause, contours suggest poleward and downward transport, being more pronounced in the Southern Hemisphere following winter. Behaviour in this lower regime is in agreement with previous results<sup>3-8</sup>. Remarkably strong gradients occur near 20° N and S to altitudes exceeding 25 km. The double ear structure seen above 23 km in QBO westerly shear (Fig. 3a) can be accounted for by weak relative upward advection of high values in the subtropics and stronger relative downward advection of low values over the Equator. Below 22 km, slight ascent is inferred over the Equator with poleward motion out to ~20°, followed by vertical divergence. A single plume is seen in QBO easterly shear during October 1988 (Fig. 3b). Lofting is inferred from 20 km to above 28 km. The elevation of the maximum rose by ~4 km over the period of a year, a phenomenon which was probably enhanced by prolonged upward aerosol transport associated with the delayed descent of the easterly shear layer (Fig. 1).

We believe that the primary features of the tropical aerosol distribution are controlled by fluid motions and that aerosol microphysical processes provide only a secondary effect except at the top of the plumes. Because temperature increases upward in the stratosphere, air parcels can ascend only if they experience net radiative heating. Aerosols evaporate as rising parcels warm, or grow in size as sinking parcels cool and water vapour condenses on the droplets. The meridional temperature variation (<5 K) associated with the QBO should cause only a slight enhancement of the observed structure. Theory predicts an extinction ratio variation of less than 10% for a temperature range of 20 K about 220 K at constant altitude with 3.5 p.p.m.v. ambient water vapour<sup>20</sup>. At the top of a plume, aerosol evaporation is probably more significant than at lower altitudes, and the aerosol distribution there is less useful for inferring the circulation.

In the upper regime, above 20 km, aerosol extinction values are much higher in the tropics than outside. This confirms the early observation<sup>8</sup> of an aerosol reservoir over the Equator following the eruption of Mount Agung (8° S, 115° E) and is compatible with the maximum in 185°W in the region a year after the 'Hardtack' bomb tests of 1958 (ref. 6). The circulation associated with the QBO tends to spread aerosols around in the tropics, and other mixing processes such as inertial instability<sup>21</sup>

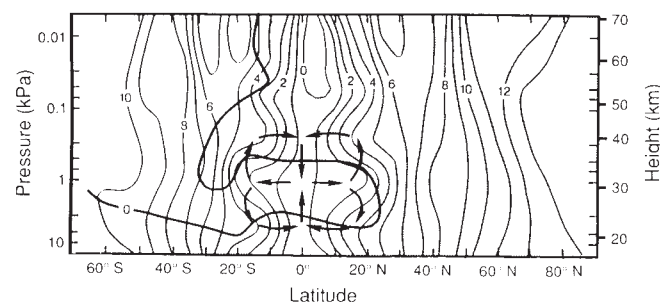


FIG. 2 Latitude-altitude section of normalized zonal mean potential vorticity (PV) derived from satellite temperature data<sup>16</sup> averaged over the period 31 October to 5 November 1978. The zero wind line separates QBO and summer easterlies from westerlies elsewhere. The arrows denote a relative meridional circulation due to the QBO which is compatible with the deformation of PV contours and the relevant theoretical models<sup>10-12</sup>. Westerly winds are shaded.

should act to homogenize aerosols in this tropical reservoir. Large gradients in aerosols and PV exist in the subtropics, but the patterns in the two are not identical. Both are in part a manifestation of the dynamics driving the QBO. Another process contributing to these gradients is mixing by planetary Rossby waves, which exist in the extratropical winter hemisphere. These waves propagate freely in westerlies (compare with Fig. 1) and cause quasi-horizontal irreversible mixing as they are absorbed<sup>22</sup>, yielding enhanced gradients on the edges of the mixing region. Their propagation is controlled by the distribution of PV. Thus it is appropriate to view the subtropical PV gradient as a semipermeable barrier to mixing by extratropical Rossby waves<sup>18</sup>. During QBO easterlies, equatorial aerosols are more effectively sequestered from poleward transport processes.

Anthropogenic and natural chemical species entering the stratosphere through the tropical tropopause might be transported poleward relatively rapidly in the lower regime. Trace gases destined for the remainder of the stratosphere would be held temporarily in the upper regime. Detrainment out of the upper reaches of the equatorial reservoir by the Brewer-Dobson circulation would occur more readily during QBO easterly shear, whereas detrainment laterally in the lower regime would occur more readily during QBO westerly shear, preferentially into the winter hemisphere.

A series of eruptions from Mount Pinatubo (18° N, 126° W)

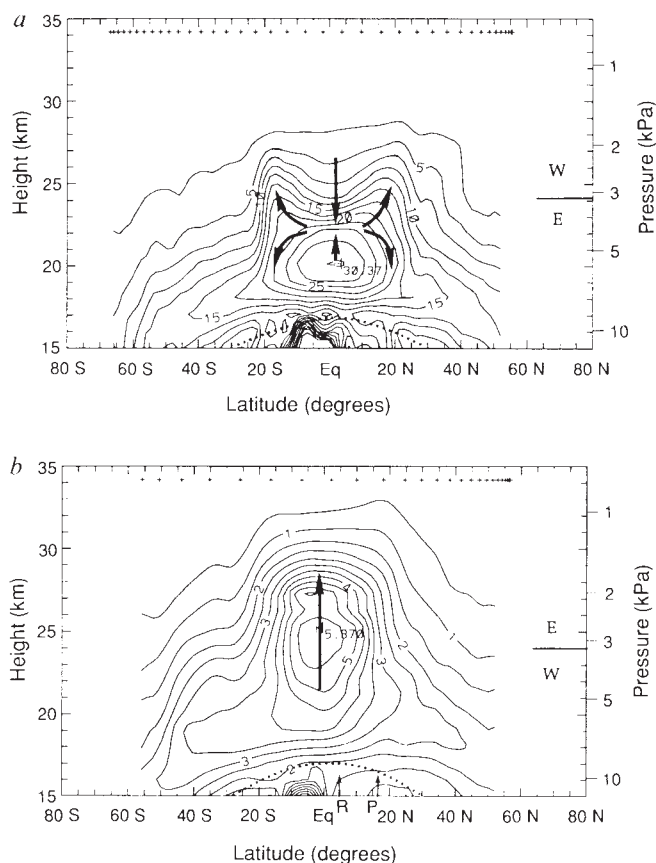


FIG. 3 Latitude-altitude cross-sections of aerosol extinction ratio at 1  $\mu\text{m}$  (refs 13, 14) during two ~40-day periods representative of two different phases of the QBO. *a*, Dominant westerly shear, centred about 11 November 1984, contour interval 2.5; *b*, dominant easterly shear, centred about 4 October 1988, with contour interval 0.5. Crosses indicate locations of the daily average of ~15 profiles. Arrows indicate the inferred QBO circulation based on the aerosol distribution. The altitude of the zero wind over the Equator is transcribed from Fig. 1 at the right of each section. The climatological tropopause is indicated by a dashed line, where cloud tops can contaminate the aerosol data. R and P indicate the latitudes of Mounts Ruiz and Pinatubo, respectively.

reached the middle stratosphere<sup>23</sup> during June 1991, a time of descending QBO easterly shear (Fig. 1). The wind structure in autumn 1991 similar to that following the eruption of Mount Ruiz (5° N, 75° W) in November 1985 and the structure in November 1988 (Fig. 3b). Recent SAGE II observations and ground-based lidar measurements indicate that Pinatubo material had already spread into the mid-latitudes of the Southern Hemisphere below 28 km and into the mid-latitudes of the Northern Hemisphere below 24 km by September 1991 (P. McCormick, personal communication). We expect that more material will be detrained into the northern mid-latitudes during winter, but as the easterly shear region reaches the lower transport regime, transport towards the poles will be less than if the shear had remained westerly. □

Received 12 August; accepted 25 November 1991.

1. Turco, R. P., Whitten, R. C. & Toon, O. B. *Rev. Geophys.* **20**, 233–279 (1982).
2. Hofmann, D. & Solomon, S. *J. geophys. Res.* **94**, 5029–5042 (1989).
3. Brewer, A. W. *Q. J. R. met. Soc.* **75**, 351–363 (1949).
4. Dobson, G. M. B. *Proc. Roy. Soc.* **A236**, 187–193 (1956).
5. Murgatroyd, R. J. & Singleton, F. Q. *J. R. met. Soc.* **87**, 125–135 (1961).
6. Feely, H. W. & Spar, J. *Nature* **188**, 1062–1064 (1960).
7. Telegadas, K. & List, R. J. *J. geophys. Res.* **74**, 1339–1350 (1969).
8. Dyer, A. J. & Hicks, B. B. *Q. J. R. met. Soc.* **94**, 545–554 (1968).
9. Reed, R. J. *Q. J. R. met. Soc.* **90**, 441–466 (1964).
10. Plumb, R. A. & Bell, R. C. *Q. J. R. met. Soc.* **108**, 335–352 (1982).
11. Dunkerton, T. J. *J. atmos. Sci.* **42**, 1151–1160 (1985).
12. Gray, L. J. & Pyle, J. A. *J. atmos. Sci.* **46**, 203–220 (1989).
13. McCormick, M. P. *et al. Bull. Am. met. Soc.* **60**, 1038–1046 (1979).
14. Russell, P. B. *et al. J. atmos. Sci.* **38**, 1295–1312 (1981).
15. Chu, W. P. *et al. J. geophys. Res.* **94**, 8339–8352 (1989).
16. Hitchman, M. H. & Leovy, C. B. *J. atmos. Sci.* **43**, 3159–3176 (1986).
17. Hoskins, B. J., McIntyre, M. E. & Robertson, A. W. *Q. J. R. met. Soc.* **111**, 877–946 (1985).
18. McIntyre, M. E. *Dynamics, Transport and Photochemistry in the Middle Atmosphere of the Southern Hemisphere* 1–18 (Kluwer, Dordrecht, 1990).
19. Haynes, P. H. & McIntyre, M. E. *J. atmos. Sci.* **44**, 828–841 (1987).
20. Yue, G. K. & Deepak, A. *Appl. Opt.* **20**, 3669–3675.
21. Andrews, D. G., Holton, J. R. & Leovy, C. B. *Middle Atmosphere Dynamics* (Academic, Orlando, 1979).
22. McIntyre, M. E. & Palmer, T. N. *J. atmos. terr. Phys.* **46**, 825–849 (1984).
23. American Geophysical Union *Eos* **72**, 305–306 (1991).
24. Naujokat, B. *et al. Beilagen zur Berliner Wetterkarte* (Free University of Berlin, 1991).

ACKNOWLEDGEMENTS. We thank P. McCormick for providing the SAGE data. We also thank M. McIntyre for conversations and P. Haynes, A. Plumb and A. Tuck for comments on the manuscript.

## Thermal disequilibrium at the top of volcanic clouds and its effect on estimates of the column height

Andrew W. Woods\* & Stephen Self†

\* Institute of Theoretical Geophysics, Department of Applied Mathematics and Theoretical Physics, Silver Street, Cambridge CB3 9EW, UK

† Department of Geology and Geophysics, School of Ocean and Earth Science and Technology, University of Hawaii at Manoa, Honolulu, Hawaii 96822, USA

SATELLITE images of large volcanic explosions reveal that the tops of volcanic eruption columns are much colder than the surrounding atmosphere<sup>1</sup>. We propose that this effect occurs whenever a mixture of hot volcanic ash and entrained air ascends sufficiently high into a stably stratified atmosphere. Although the mixture is initially very hot, it expands and cools as the ambient pressure decreases. We show that cloud-top undercoolings in excess of 20 °C may develop in clouds that penetrate the stratosphere; this is consistent with observations of the 4 April 1982 eruption of El Chichón<sup>1</sup> and the 18 May 1980 eruption of Mount St Helens<sup>2</sup>. Furthermore, from our model results, we predict that for a given cloud-top temperature, variations in the initial temperature of 100–200 °C may correspond to variations in the column height of 5–10 km. We deduce that the present practice of converting satellite-based measurements of the temperature at the top of volcanic eruption columns to estimates of the column height will produce rather inaccurate results and should therefore be discontinued.

Many of the hazards associated with explosive volcanic eruptions result from the vast clouds of ash which are injected tens of kilometres into the atmosphere. During an eruption, the ash cloud is a danger to aircraft flying near the volcano. During both the eruption of Redoubt, Alaska on 15 December 1989 and the eruption of Pinatubo, Philippines on 15 June 1991, several commercial aircraft flew into ash clouds, leading to temporary in-flight engine failure and considerable damage to the aircraft. So that aircraft can be re-routed, accurate predictions of the location of the ash clouds are required. A key element of any such prediction is knowledge of the eruption column height, particularly because the prevailing winds which disperse the ash often change direction with altitude. Accurate information about the height of rise of the cloud also allows better estimates of both the geographical extent of ash deposits<sup>3–6</sup> and the long-term climatic impact of an eruption, resulting from sulphuric acid aerosols injected into the stratosphere<sup>7</sup>.

It has been the practice to determine the altitude of volcanic clouds by obtaining cloud-top temperature from a thermal-infrared sensor on a satellite and equating this with the ambient atmospheric temperature obtained from radiosondes on balloon launches<sup>1,8–10</sup>. But this method has been shown either to give unrealistic cloud altitudes which differ from independent measurements of cloud height or to give cloud temperatures slightly colder than the temperature at any height in the atmosphere<sup>1,8–11</sup>. Such differences in temperature were not noted to be significant. In several recent large volcanic eruptions (Table 1), however, satellite-perceived cloud-top temperatures have been consistently lower than the temperature of the surrounding atmosphere at that altitude. As far as we are aware, no explanation of this paradox has been proposed. Matson<sup>1</sup> has suggested that his data might be explained by assuming the cloud spreads out laterally at the tropopause, where the ambient temperature has its minimum, even though this minimum may still be a few degrees greater than the cloud-top temperature. We believe that this interpretation is inconsistent with data from the 4 April 1982 'C' phase plume of El Chichón. Images obtained from a GOES satellite, 90 and 120 min after the eruption, show the cloud top had cooled to –82 °C. Independent estimates from numerical models of fallout<sup>6</sup> and from the wind fields<sup>1</sup> suggest that the cloud ascended to an altitude of 26 ± 3 km. But radio-sonde data from the two nearest Mexican stations, Merida and Veracruz, show the ambient temperatures at altitudes of 26 ± 3 km were in the range –55 to –40 °C. Therefore, at the cloud-top, the ambient temperature was 20–35 °C warmer than the cloud. Indeed, the cloud-top was a few degrees colder than the tropopause (–76 °C) but the tropopause was located at an altitude of 17 km, nearly 10 km below the cloud top.

Our purpose here is to explain and quantify these observations, and thereby predict bounds on the column height as a function of satellite-perceived cloud-top temperatures. The difference in temperature between the relatively cold volcanic cloud tops and the surrounding atmosphere may be understood by considering a simple buoyant plume in a stratified environment<sup>12</sup>. Relatively warm fluid, released from a nozzle into a thermally stratified fluid, convects upwards towards the neutral buoyancy height, at which the plume density and hence temperature equal those of the environment. The inertia of the plume fluid then carries it upwards above the neutral buoyancy height, until it has decelerated to rest under gravity. Therefore, at its maximum height, a simple plume is in fact colder than the ambient.

In a volcanic cloud, the situation is more complex. Volcanoes erupt dense, hot mixtures of ash and clasts, at high speed. This mixture entrains ambient air, which is heated and expands, and thereby a buoyant mixture of ash and gas<sup>13–15</sup> is generated. This buoyant mixture rises into the atmosphere and, as in a simple plume, ascends beyond its neutral buoyancy height where its bulk density equals that of ambient. But a volcanic eruption column contains dense ash particles, and so at the neutral